The Egyptian Journal of Radiology and Nuclear Medicine (2014) **45**, 619–626

Egyptian Society of Radiology and Nuclear Medicine

The Egyptian Journal of Radiology and Nuclear Medicine

www.elsevier.com/locate/ejrnm
www.sciencedirect.com

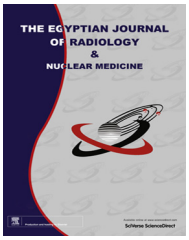

REVIEW

MRI evaluation of fatty liver in day to day practice: Quantitative and qualitative methods

Kiran Gangadhar [*], **Kedar N. Chintapalli** [1], **Gilbert Cortez** [1], **Sandhya Vinu Nair** [1]

Department of Body Imaging and Intervention, UTHSCSA, San Antonio, TX, USA

Received 2 March 2014; accepted 16 May 2014
Available online 10 June 2014

KEYWORDS

Hepatic steatosis;
Non-alcoholic fatty liver disease;
MRI liver;
MRI methods;
Chemical shift imaging

Abstract Intracellular fat accumulation is a common feature of liver disease. Steatosis is the histological hallmark of non-alcoholic fatty liver disease (NAFLD) but also may occur with alcohol abuse, viral hepatitis, HIV and genetic lipodystrophies, and chemotherapy. This condition is common in the Western population and is typically associated with obesity and the metabolic syndrome. Early diagnosis and early treatment of NAFLD are important to prevent the development of end-stage liver disease and cancer. In addition, liver fat is a risk factor for postoperative complications after liver resection and transplantation. MRI has become a primary modality to assess hepatic steatosis, both qualitatively and quantitatively. In this article we discuss various MRI methods for evaluation of hepatic steatosis.

Contents

1. Introduction 620
2. Chemical shift imaging (dual echo) 620
3. Multi-echo Dixon sequences 621
4. MR spectroscopy 624
5. Conclusion 625

Abbreviations: BMI, body mass index; NAFLD, nonalcoholic fatty liver disease; NASH, nonalcoholic steatohepatitis; PDFF, proton density fat fraction; MRI, magnetic resonance imaging; MRS, magnetic resonance spectroscopy; GRE, gradient echo; TE, echo time; TR, repetition time; USG, ultrasonography; LFT, liver function tests.

* Corresponding author. Address: 4900 Medical Drive, #811, San Antonio, TX, USA. Tel.: +1 314 262 3552.
E-mail addresses: kirang.585@googlemail.com, gangadhar@uthscsa.edu (K. Gangadhar), chintapalli@uthscsa.edu (K.N. Chintapalli), cortezG3@uthscsa.edu (G. Cortez), VinuNair@uthscsa.edu (S.V. Nair).
[1] 7703 Floyd Curl Dr San Antonio, TX 78229, USA.

Peer review under responsibility of Egyptian Society of Radiology and Nuclear Medicine.

 http://dx.doi.org/10.1016/j.ejrnm.2014.05.015

Authors' contributions . . . 625
Conflict of interest . . . 625
Disclosures . . . 625
Consent . . . 625
Human and animal rights . . . 626
Acknowledgements . . . 626
References . . . 626

1. Introduction

Fatty liver disease refers to a spectrum of conditions characterized by accumulation of increasing amounts of triglycerides within the hepatocyte. There is a wide variation in incidence rates for NAFLD (1). An estimated prevalence of 25–35% is seen in the general population of the United States (2). Whereas, a study from Greece revealed evidence of steatosis in 31% and NASH in 40% of autopsied cases of ischemic heart disease or traffic accident death after exclusion of hepatitis B seropositivity or known liver disease (3). The prevalence of fatty liver disease is higher among those who consume large quantities (>60 g per day) of alcohol (45%), those with hyperlipidemia (50%) or obesity (body mass index, >30 kg/m^2) (75%), and those with both obesity and high alcohol consumption (95%) (4).

The exact pathogenesis of NAFLD remains poorly understood. The current hypothesis by experts in the field is that several insults are involved in causing progressive liver injury (5). With the initial hit, macrovesicular steatosis results. Insulin resistance (6) most likely plays a central role in the net retention of lipids, particularly triglycerides, within the hepatocytes. Although the mechanisms have not been completely elucidated, this is thought to result from decreased disposal of fatty acids due to impaired mitochondrial β-oxidation (7). The second insult is generally due to oxidative stress, which causes peroxidation of lipids in the hepatocyte membrane, cytokine production, and Fas ligand induction (8) and is in large part responsible for the progression from steatosis to NASH to cirrhosis. Bacterial toxins (9), overproduction of cytokines (especially tumor necrosis factor-α) (10), and alteration of hepatocyte ATP stores and cytochrome P450 Cyp2E1/Cyp4A enzyme activity (11) are also considered as potential triggers for disease progression and fibrogenesis.

Furthermore, hepatic steatosis has been reported to affect the progression of various chronic liver diseases. For example, hepatic steatosis has been found to adversely affect the progression of hepatic fibrosis and the response to antiviral treatment in patients with hepatitis C (12–14). Moreover, hepatic steatosis has been found to be an important cofactor in liver injury observed in patients with hemochromatosis and alcoholic liver disease. Therefore, the assessment of hepatic steatosis may have important clinical implications in the management of patients with chronic liver disease (15). In order to grade steatosis, pathologists visually estimate the fraction of hepatocytes that contain fat droplets. Typically, a five-point ordinal scale is used (0%, 1–5%, 6–33%, 34–66%, or >67%). The size of fat droplets is not considered (16). However, most agree that a very mild degree of steatosis involving less than 5% of hepatocytes may not actually represent a true pathologic abnormality (2).

MRI is an attractive modality to assess hepatic steatosis. In and out of phase MRI, calibrated with robust liver/fat standards, have been found to be superior in quantifying hepatic steatosis, when compared with non-invasive methods (17). Advanced MRI techniques currently under development have demonstrated high potential for accurate detection and quantification of hepatic steatosis using proton density fat-fraction (18). MR imaging (chemical shift imaging, multi-echo Dixon method) and MR spectroscopy for quantifying liver fat will be discussed in later sections.

2. Chemical shift imaging (dual echo)

On MRI, fatty liver has high signal intensity on T1-weighted images. In addition, several MRI sequences, including fat-suppression sequences and chemical shift imaging with OP gradient recalled echo sequences facilitate the detection of fat (19). The magnitude-based approach is probably the most commonly used MR approach for liver fat assessment in current practice. Typically, two gradient echoes are acquired, one employing a TE in which the water peak (4.7 ppm) and the dominant fat peak (1.3 ppm) are "out of phase" and hence subtractive, and the other using a TE in which the two peaks are "in phase" and therefore additive. Because two echoes are acquired, this is often called "dual-phase" or "dual echo" imaging. The TE corresponding to in-phase and out-of-phase (IOP) depend on the magnet field strength. At 1.5 T, the chemical shift between water and the dominant fat peak (3.4 ppm) corresponds to a resonance frequency difference of 217 Hz (i.e. the main fat peak resonates 217 Hz slower than the water peak). Therefore, at 1.5 T, signals from water and the main fat peak oscillate with a period of 4.6 ms (1000 ms/217 Hz). At 3 T, the chemical shift corresponds to a frequency difference of 434 Hz (double that at 1.5 T). Therefore, the oscillation period at 3 T (2.3 ms) is half that at 1.5 T (4.6 ms) and the corresponding IP and OP echo times at 3 T are halved: water and the main fat peak are in phase every 2.3 ms (i.e., 2.3, 4.6, and 6.9 ms) and out of phase at 1.15 ms and every subsequent multiple of 2.3 ms (i.e., 1.15, 3.45, and 5.75 ms) (20).

To estimate the signal fat-fraction, we assume (1) the signal intensity from fat is less than the signal intensity from water (i.e. $S_{\mathrm{Fat}} \leqslant \mathrm{SI}_{\mathrm{Water}}$); (2) the signal intensity from OP images represents the difference in water and fat signals (i.e., $S_{\mathrm{OP}} = S_{\mathrm{Water}} - S_{\mathrm{Fat}}$); and (3) the signal intensity from IP images represents the sum of water and fat signals (i.e., $S_{\mathrm{IP}} = [S_{\mathrm{Water}} + S_{\mathrm{Fat}}]$) (21). Fat Signal Percentage is calculated as $[S_{\mathrm{IP}} - S_{\mathrm{OP}}]/[2 \times \mathrm{SIP}] \times 100$. The dynamic range of magnitude-based chemical shift techniques has typically a 0–50% signal fat-fraction (Figs. 1–3) (18).

The use of MR imaging with the chemical shift imaging for the detection and quantification of fatty liver provides the

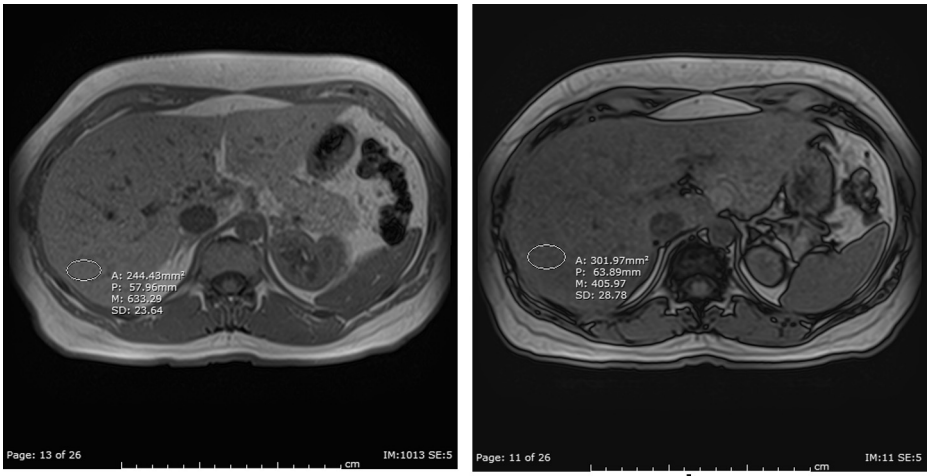

Fig. 1 A 37 year old female with vague abdominal pain, evaluation of hypoechoic lesion found on recent USG. (a) In-phase GRE and (b) opposed-phase GRE images showing mild hepatic steatosis with signal drop on opposed phase images. Percentage fat fraction corresponding to 22%.

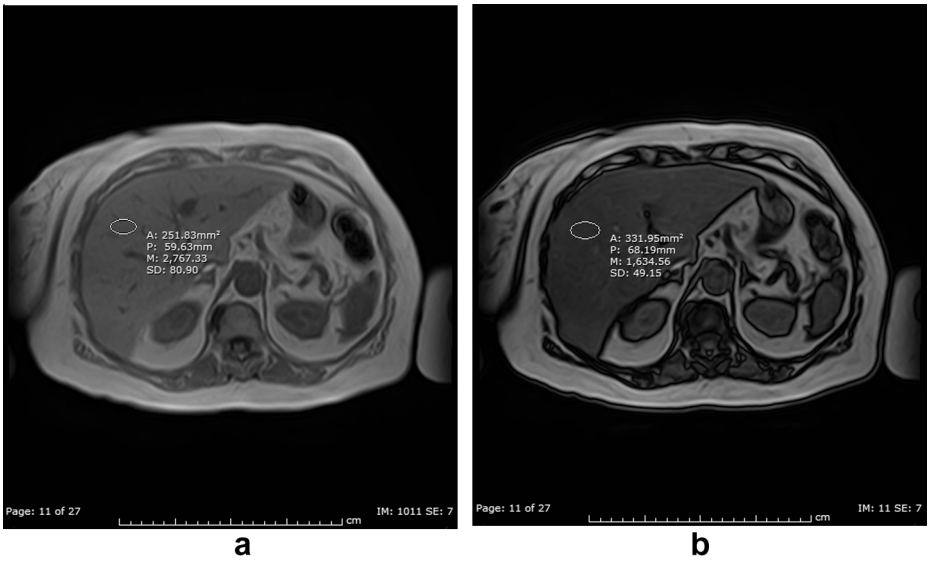

Fig. 2 A 49 year old female with elevated LFT, biliary duct dilation, prior cholecystectomy and MR imaging done to rule out choledocholithiasis. (a) In-phase GRE and (b) opposed-phase GRE images showing moderate hepatic steatosis with moderate signal drop on opposed phase images. Percentage fat fraction corresponding to 30%.

following benefits: (a) technical simplicity, (b) coverage of the entire liver, (c) minimal vulnerability to confounding factors, and (d) absence of radiation exposure. Limitations to the routine use of MR imaging in liver fat quantification include potential variability of results due to differences in MR imaging systems, scanning parameters, and methods of analysis (2).

3. Multi-echo Dixon sequences

This technique uses both magnitude and phase information from three or more images acquired at echo times appropriate for more accurate separation of water and fat signals (based on the identification of 3 fat peaks, rather than the commonly used single dominant fat peak, to optimize separation of water and fat signals) (22–26).

These methods provide estimates of fat fraction with a dynamic range of 0–100%. While this dynamic range of 0–100% is important for imaging adipose tissue (27), it may not be necessary for quantifying the hepatic proton density fat fraction, which infrequently exceeds 50%. In addition to correction for T1, $T2^*$ and the spectral complexity of fat, complex-based MRI methods also require correction for noise bias and eddy currents.

Noise bias occurs if magnitude of water and fat images are recombined, because areas of low signal (e.g. fat signal from a liver with no fat) have only positive noise after the magnitude operation. Methods that create fat-fraction maps from

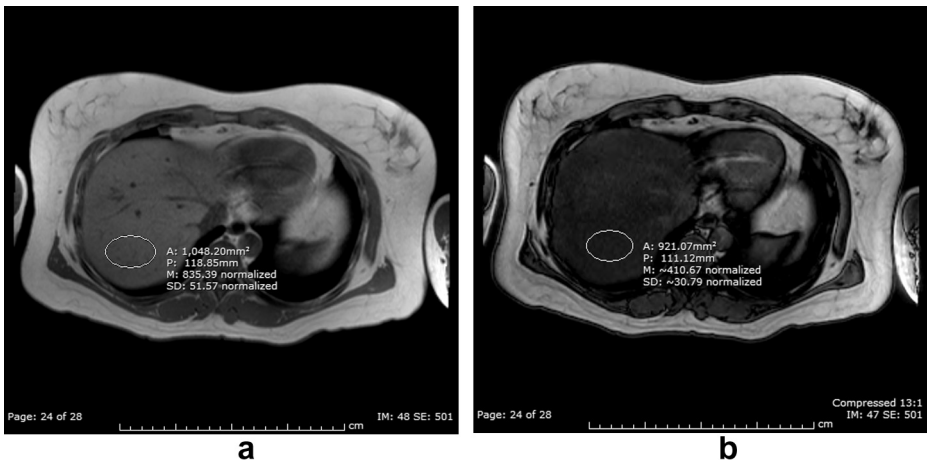

Fig. 3 A 46 year old female with right upper quadrant discomfort and elevated liver enzymes. (a) In-phase GRE and (b) opposed-phase GRE images showing severe hepatic steatosis with severe signal drop on opposed phase images. Percentage fat fraction corresponding to 43%.

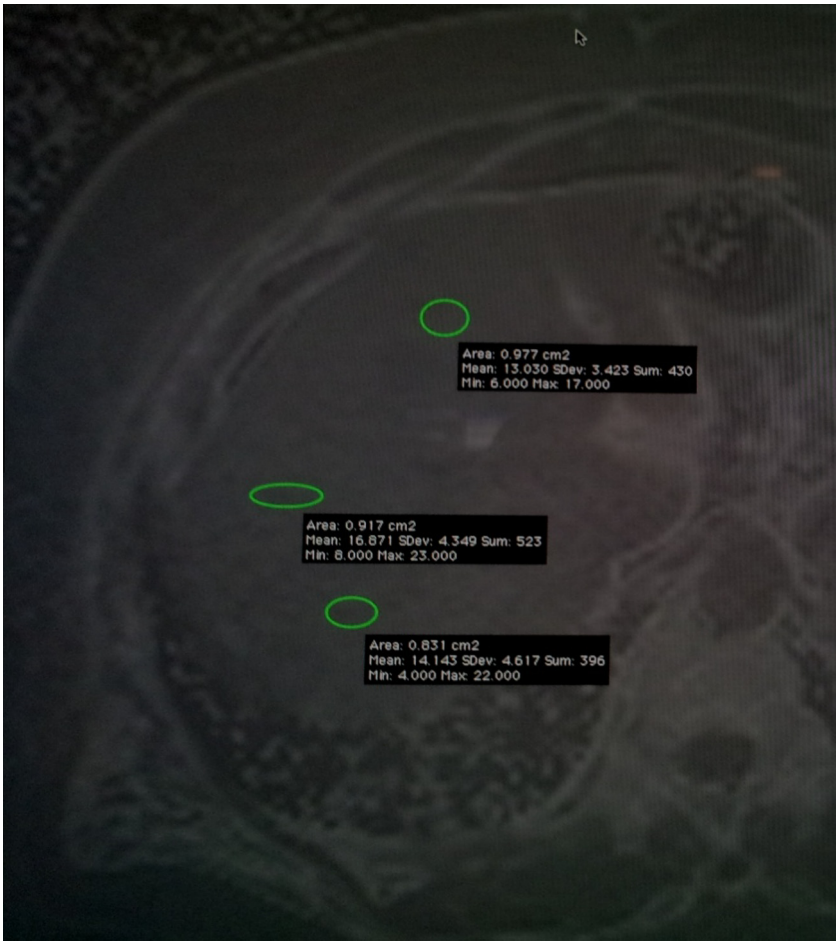

Fig. 4 A 33 year old male, MR imaging was done for renal cyst evaluation. PDFF map showing mild hepatic steatosis with average PDFF value of 16 units.

in-phase and opposed-phase images are more immune to these effects except near fat-fractions of 50% when the signal intensity of opposed-phase images approaches zero and noise bias impacts fat-fraction calculations. Since low fat-fractions (near zero) are more clinically relevant, noise bias effects are more important in chemical shift based water-fat separation methods (25).

Rapidly switching gradients lead to phase shifts on complex images acquired at different echo times. These phase shifts can corrupt estimates of fat-fraction. Eddy currents affect methods

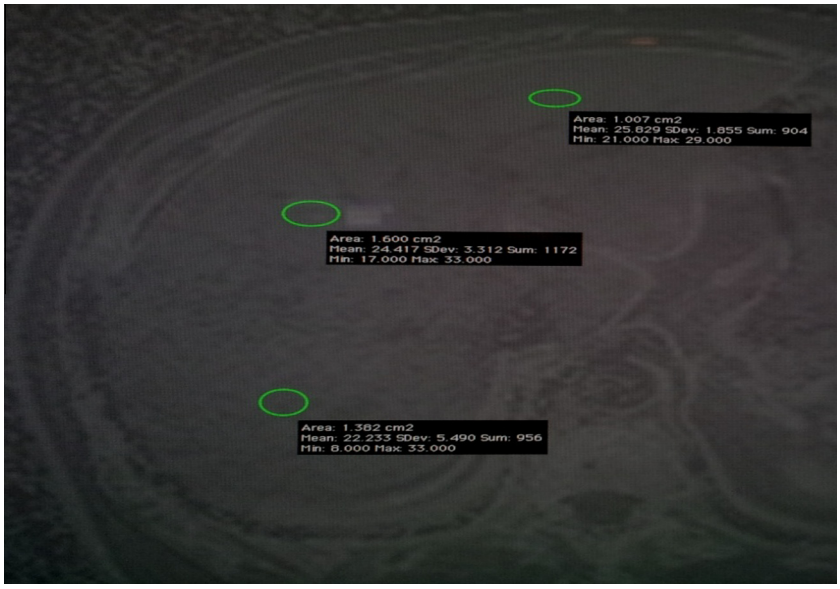

Fig. 5 Obese female, MR imaging was done for elevated liver enzymes and recurrent abdominal pain. PDFF map showing moderate hepatic steatosis with average PDFF value of 22 units.

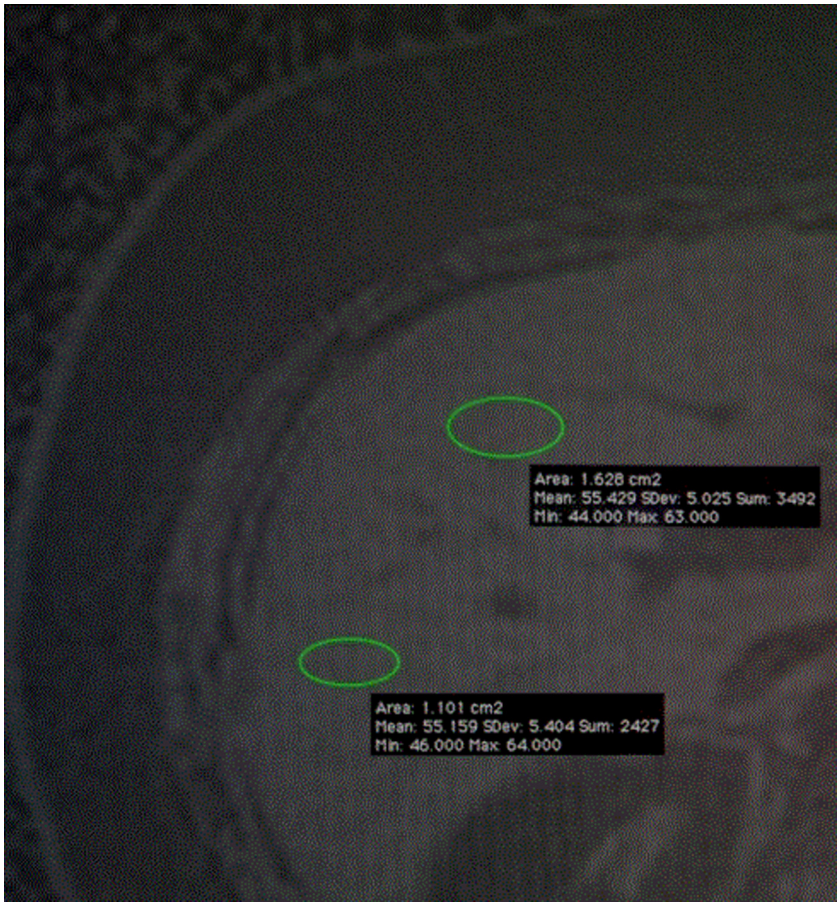

Fig. 6 A 44 year old male with chronic hepatitis C for routine surveillance. PDFF map showing severe hepatic steatosis with average PDFF value of 55 units.

that use phase information in images acquired at different echo times to quantify fat such as chemical shift based water-fat separation methods. Correction for eddy current can be performed using a hybrid complex-magnitude approach recently reported by Yu et al. (26). Importantly, magnitude-based methods, including conventional IOP imaging and other

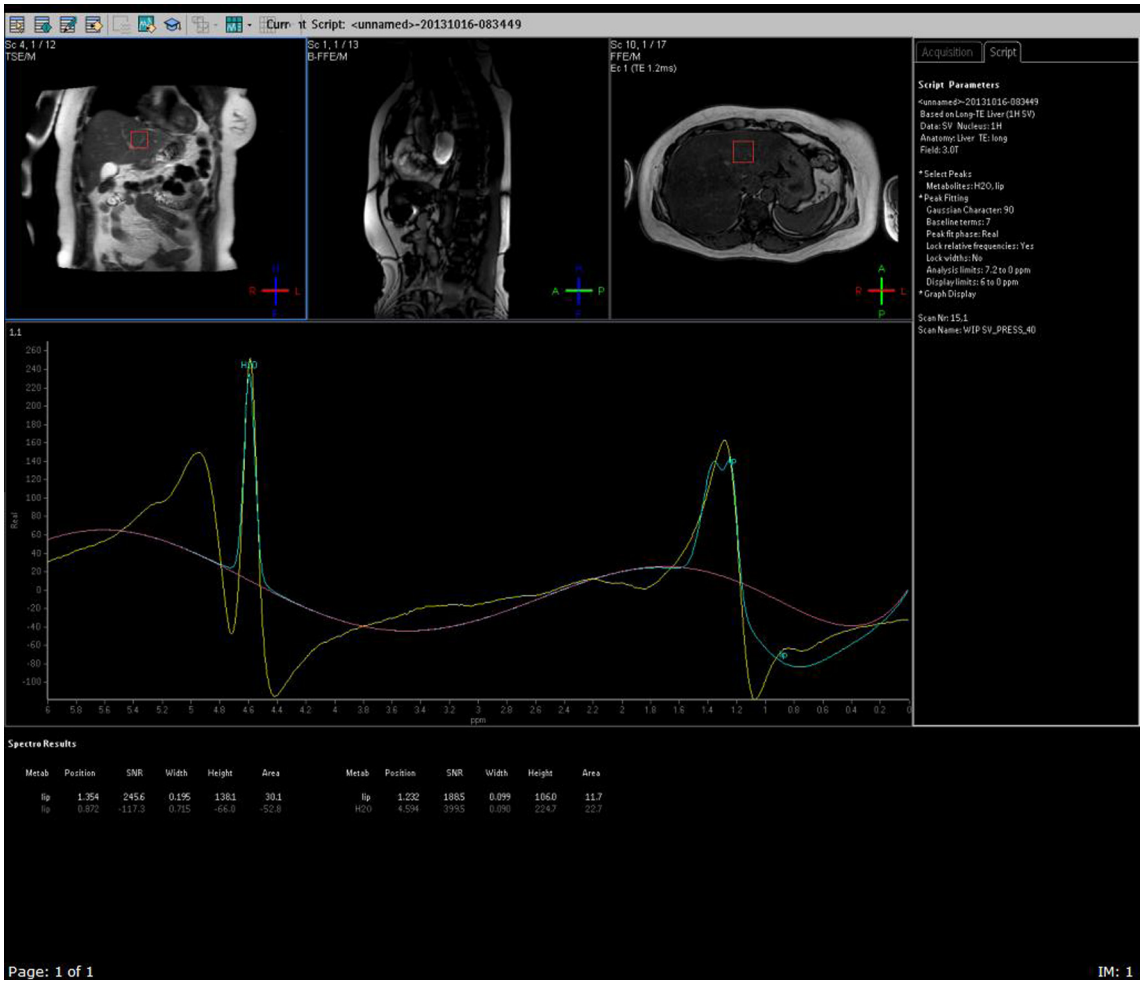

Fig. 7 A 46 year old male patient with chronic hepatitis C and elevated liver function tests, MRS with single voxel in 3 T MRI showing moderate hepatic steatosis with increased lipid peak (marked as 'lp'), which is nearing the level of water peak (marked as 'H_2O').

magnitude-based methods discard all phase information and should be relatively immune to the effects of eddy currents (18).

This technique utilizes a gradient echo sequence with low flip angles (FA) to minimize T1 bias, and acquires multiple echoes at echo times at which fat and water signals are nominally in-phase or out-of-phase relative to each other. Data obtained at each of the echo times are passed to a nonlinear least-squares fitting algorithm that estimates and corrects $T2^*$ effects, models the fat signal as a superposition of multiple frequency components, and estimates fat and water proton densities from which the fat content is calculated. Using custom analysis software, the mathematical model is applied pixel-by-pixel on the source images to generate parametric PDFF maps that depict the quantity and distribution of fat throughout the entire liver. Imaging PDFF (Figs. 4–6) are recorded in region of interest (ROI) areas placed on the PDFF parametric maps, avoiding vessels, bile ducts, lesions and artifacts (28).

The multi-echo method estimates FF and $T2^*$ time using three pairs of OP and IP echoes. This method simultaneously estimates signal intensities of the fat and water components and the $T2^*$ relaxation times by using least-square fitting of all six echoes as a function of the equation $SI = |S_w + S_f e^{2piDfTE}|e^{-TE/T2^*}$, where S_w = SI of the water component, S_f = SI of the fat component, Df = frequency difference between water and methylene protons of fatty acids, i.e. 210 Hz at 1.5 T (27). FF is calculated as $S_f/(S_w + S_f)$.

4. MR spectroscopy

MRI and magnetic resonance spectroscopy (MRS) provide non-invasive means to accurately quantify intrahepatic lipid content (29–31). In contrast to other modalities such as ultrasound and computed tomography (CT), MRI/MRS is capable of detecting even small amounts of intrahepatic lipid accumulation (31). Therefore, MRI/MRS is especially useful to measure changes in hepatic steatosis during various treatment regimens. During recent years, clinical and research investigations have been performed on this subject (32).

In MRS, signals from chemicals in tissue or metabolites are recorded. The metabolite peaks are identified primarily by their frequencies (i.e., their position in the spectrum) and are expressed as a shift in frequency (in parts per million [ppm]) relative to a standard of water. The most common nuclei used for in vivo MR spectroscopy are protons (^1H), sodium (^{23}Na), and phosphorus (^{31}P). The advantages of ^1H spectroscopy are

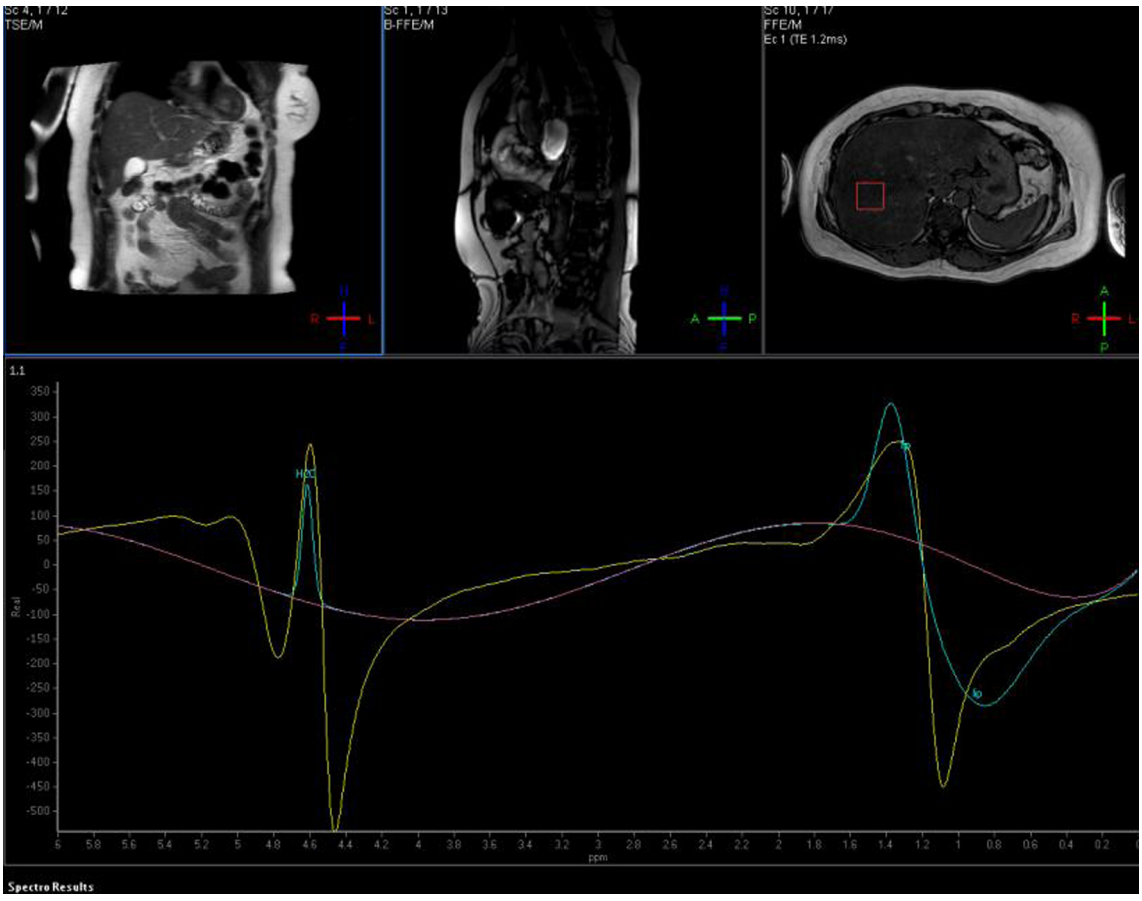

Fig. 8 A 43 year old female patient with right upper quadrant discomfort with elevated liver function tests, MRS with single voxel in 3 T MRI showing severe hepatic steatosis with increased lipid peak (marked as 'lp') as compared to water peak (marked as 'H_2O').

that it is easier to perform, it is more widely available, and it provides a much higher signal-to-noise ratio (SNR) than is the case with ^{23}Na and ^{31}P. In ^{1}H MR spectroscopy, the frequency location of a metabolite or chemical compound depends on the configuration of the protons within the chemical (33).

Two main strategies are used for single-voxel spectroscopy (SVS) (Figs. 7 and 8) where individual voxels are analyzed: point-resolved spectroscopy (PRESS) or stimulated-echo acquisition mode (STEAM) (34). The PRESS acquisition scheme (multi-echo single-shot technique) uses a 90°–180°–180° pulse sequence with a long echo time (TE) and allows for a better visualization of metabolites with long T1-relaxation times. In contrast, the STEAM sequence applies a 90°–90°–90° pulse sequence and is less sensitive to *J*-coupling effects, dipole–dipole coupling or spin–spin coupling. The STEAM sequence provides shorter TE and lower signal yield compared to PRESS, which is usually not a practical limitation in fat quantification in the liver. Both techniques can be applied in intrahepatic fat quantification in clinical examinations (35).

5. Conclusion

MR imaging is a very sensitive and specific noninvasive modality for detection of hepatic steatosis. Chemical shift images are an efficient method for screening, diagnosis and semiquantification of liver steatosis. Multi-echo Dixon MR imaging, as proven by some recent studies, provides a technique for quantifying liver fat content using proton density fat fraction that is highly correlated with MRS, which in turn has great correlation with tissue diagnosis as proven by many studies. Thus, MR imaging is a versatile modality for hepatic quantification and helps in avoiding unnecessary random liver biopsies.

Authors' contributions

The author is involved in case collection and documentation.

Conflict of interest

There is no conflict of interest to declare.

Disclosures

Nil.

Consent

Yes.

Human and animal rights

Not applicable.

Acknowledgements

We would like to thank Shwetha, and Deepa for their kind support and encouragement.

References

(1) Vernon G, Baranova A, N.N. Younoss. Systematic review: the epidemiology and natural history of non-alcoholic fatty liver disease and non-alcoholic steatohepatitis in adults. Aliment Pharmacol Ther 2011;34:274–85.
(2) Xiaozhou Ma, Holalkere Nagaraj-Setty, et al. Imaging-based quantification of hepatic fat: methods and clinical applications. RadioGraphics 2009;29:1253–80.
(3) Zois CD, Baltayiannis GH, Bekiari A, et al. Steatosis and steatohepatitis in postmortem material from Northwestern Greece. World J Gastroenterol 2010;16:3944–9.
(4) Okka W, Hamer MD, et al. Fatty liver: imaging patterns and pitfalls. RadioGraphics 2006;26:1637–53.
(5) Day CP, James OF. Steatohepatitis: a tale of two "hits"? Gastroenterology 1998;114(4):842–5.
(6) Tominaga K, Kurata JH, Chen YK, et al. Prevalence of fatty liver in Japanese children and relationship to obesity. An epidemiological ultrasonographic survey. Dig Dis Sci 1995;40(9): 2002–9.
(7) Reid AE. Nonalcoholic steatohepatitis. Gastroenterology 2001;121(3):710–23.
(8) Pessayre D, Berson A, Fromenty B, Mansouri A. Mitochondria in steatohepatitis. Semin Liver Dis 2001;21(1):57–69.
(9) Yang SQ, Lin HZ, Lane MD, Clemens M, Diehl AM. Obesity increases sensitivity to endotoxin liver injury: implications for the pathogenesis of steatohepatitis. Proc Natl Acad Sci U S A 1997;94(6):2557–62.
(10) Kern PA, Saghizadeh M, Ong JM, Bosch RJ, Deem R, Simsolo RB. The expression of tumor necrosis factor in human adipose tissue. Regulation by obesity, weight loss, and relationship to lipoprotein lipase. J Clin Invest 1995;95(5):2111–9.
(11) Leclercq IA, Farrell GC, Field J, Bell DR, Gonzalez FJ, Robertson GR. CYP2E1 and CYP4A as microsomal catalysts of lipid peroxides in murine nonalcoholic steatohepatitis. J Clin Invest 2000;105(8):1067–75.
(12) Cheung O, Sanyal AJ. Hepatitis C infection and non-alcoholic fatty liver disease. Clin Liver Dis 2008;12:573–85, viii–ix.
(13) Powell EE, Jonsson JR, Clouston AD. Steatosis: co-factor in other liver diseases. Hepatology 2005;42:5–13.
(14) Gordon A, McLean CA, Pedersen JS, Bailey MJ, Roberts SK. Hepatic steatosis in chronic hepatitis B and C: predictors, distribution and effect on fibrosis. J Hepatol 2005;43:38–44.
(15) Lee Seung Soo et al. Hepatic fat quantification using chemical shift MR imaging and MR spectroscopy in the presence of hepatic iron deposition: validation in phantoms and in patients with chronic liver disease. J Magn Reson Imaging 2011;33: 1390–8.
(16) Scheuer PJ, Lefkowitch JH. Fatty liver and lesions in the alcoholic. In: Liver biopsy interpretation. Philadelphia (PA): Saunders; 2000. p. 111–29.
(17) Dimitri Aristotle Raptis, Michael Alexander Fischer, et al. MRI: the new reference standard in quantifying hepatic steatosis? Gut 2012; 61: e117–e127. doi: 10.1136/gutjnl-2011-300155.
(18) Reeder et al. Quantitative assessment of liver fat with magnetic resonance imaging and spectroscopy. J Magn Reson Imaging 2011;34:729–49.
(19) Westphalen AC, Qayyum A, Yeh BM, et al. Liver fat: effect of hepatic iron deposition on evaluation with opposed-phase MR imaging. Radiology 2007;242:450–5.
(20) O'Regan Martina F. Callaghan, Marzena Wylezinska-Arridge, et al. Simultaneous measurement by using breath-hold multiecho MR imaging at 3.0 T—feasibility. Radiology 2008; 247.
(21) Dixon WT. Simple proton spectroscopic imaging. Radiology 1984;153:189–94.
(22) Reeder SB, McKenzie CA, Pineda AR, et al. Water–fat separation with IDEAL gradient-echo imaging. J. Magn Reson Imaging 2007;25(3):644–52.
(23) Kim H, Taksali SE, Dufour S, et al. Comparative MR study of hepatic fat quantification using single-voxel proton spectroscopy, two-point Dixon and three-point IDEAL. Magn Reson Med 2008;59(3):521–7.
(24) Kovanlikaya A, Guclu C, Desai C, Becerra R, Gilsanz V. Fat quantification using three-point Dixon technique: in vitro validation. Acad Radiol 2005;12(5):636–9.
(25) Liu CY, McKenzie CA, Yu H, Brittain JH, Reeder SB. Fat quantification with IDEAL gradient echo imaging: correction of bias from T(1) and noise. Magn Reson Med 2007;58(2): 354–64.
(26) Yu H, Shimakawa A, McKenzie CA, Brodsky E, Brittain JH, Reeder SB. Multiecho water–fat separation and simultaneous R2* estimation with multifrequency fat spectrum modeling. Magn Reson Med 2008;60(5):1122–34.
(27) Bornert P, Keupp J, Eggers H, Aldefeld B. Whole-body 3D water/fat resolved continuously moving table imaging. J Magn Reson Imaging 2007;25(3):660–5.
(28) Permutt Z, Le T-A, Peterson MR, Seki E, et al. Correlation between liver histology and novel magnetic resonance imaging in adult patients with non-alcoholic fatty liver disease. Aliment Pharmacol Ther 2012;36(1):22–9.
(29) Sijens PE. Parametric exploration of the liver by magnetic resonance methods. Eur Radiol 2009;19:2594–607.
(30) Mehta SR, Thomas EL, Bell JD, Johnston DG. Taylor Robinson SD. Non-invasive means of measuring hepatic fat content. World J Gastroenterol 2008;14:3476–83.
(31) Schwenzer NF, Springer F, Schraml C, Stefan N, Machann J, Schick F. Non-invasive assessment and quantification of liver steatosis by ultrasound, computed tomography and magnetic resonance. J Hepatol 2009;51:433–45.
(32) Fabian Springer, Jürgen Machann, Claus D Claussen, Fritz Schick, et al. Liver fat content determined by magnetic resonance imaging and spectroscopy. World J Gastroenterol 2010;16(13): 1560–6.
(33) Qayyum Aliya. MR spectroscopy of the liver: principles and clinical applications. RadioGraphics 2009;29:1653–64.
(34) Angulo P, Keach JC, Batts KP, Lindor KD. Independent predictors of liver fibrosis in patients with nonalcoholic steatohepatitis. Hepatology 1999;30:1356–62.
(35) Gramlich T, Kleiner DE, McCullough AJ, Matteoni CA, Boparai N, Younossi ZM. Pathologic features associated with fibrosis in nonalcoholic fatty liver disease. Hum Pathol 2004;35:196–9.